V International Conference on Particle-based Methods – Fundamentals and Applications
PARTICLES 2017
P. Wriggers, M. Bischoff, E. Oñate, D.R.J. Owen, & T. Zohdi (Eds)

A STABLE, IMPLICIT TIME INTEGRATION SCHEME FOR DISCRETE ELEMENT METHOD AND CONTACT PROBLEMS IN DYNAMICS

ROY LICHTENHELDT[1]

[1] German Aerospace Center (DLR) - Institute of System Dynamics and Control
Münchener Straße 20, 82234 Weßling, Germany
Roy.Lichtenheldt@dlr.de, www.dlr.de/sr

Key words: Granular Material, DEM, Integration, Solver, Contact Problems, Soil, Regolith

Abstract. The field of applications for Discrete Element Method is constantly growing, enabling the simulation of granular matter. However state of the art integration schemes are mostly adopted from other methods, which results in certain drawbacks in either performance and/or accuracy. The most common time integration schemes in Discrete Element Method are explicit algorithms which are conditionally stable, only. Attempts to use implicit schemes usually require evaluation of the right hand side of the equations of motion, i.e. a complete reevaluation of the neighborhood search and contact forces within predictor-corrector iterations. While both are most suitable for simulations of rapid flows, computational efficiency is sacrificed for simulations of dense granular matter. The algorithm presented in this paper is a predictor-corrector scheme using a prediction of the forces, without evaluating the right hand side, to get an implicit estimate for the next time step. This technique enables to speed up particle simulation while using considerably higher time steps. The usage of the algorithm and the correspondent time step control are shown in example problems and accuracy is verified.

1 INTRODUCTION

The rapid increase in computational performance enabled a rapid growth of Discrete Element Method (DEM) in a wide range of applications. As the method itself is still computational expensive, most research is focused on the applications themselves, leaving the method with several drawbacks [1]. One of these is the use of non-specialized time integration schemes. The most commonly used Verlet and Leapfrog integration schemes as well as their derivatives are explicit schemes, featuring conditional stability only. Hence their maximum time step is limited by a critical time step, calculated from the highest

eigen frequency of the system. According to [2], this yields:

$$\Delta t_{\max} = \min\left(r_{\mathrm{P}}\sqrt{\frac{\rho_{\mathrm{P}}}{E}}\right) \tag{1}$$

with $r_{\mathrm{P}}, \rho_{\mathrm{P}}, E$ being the radii, density and YOUNG's Modulus of the particles. These time steps easily reach regions of $[10^{-8}, 10^{-7}]$s for realistic parameter sets, like given in [1]. Implicit integration schemes, like the NEWMARK-β integrator implemented in Pasimodo [3, 4] are unconditionally stable for continuous forces [4], but only conditionally stable for the non-continuous nature of contact forces [5]. However their critical time step size for non-continuous forces is way bigger than the explicit one. Given that high-frequency oscillations are not important for the results accuracy in many applications like soil modeling, the critical time step evaluates to [5]:

$$\Delta t_{\max} \leq S_{\mathrm{f}} \cdot \frac{\delta_{\max}}{|\vec{v}_{\max}|} \tag{2}$$
$$\text{with } \delta_{\max} = |\vec{u}_{\mathrm{dyn}}| \cdot r_{\mathrm{P}}; \quad |\vec{u}_{\mathrm{dyn}}| \in [0.05; 0.1]$$

whereas $\vec{v}_{\max}$ is the maximum expected velocity of any particle in the simulation scenario, $\delta_{\max}$ is the maximum allowed overlap in soft sphere DEM and $\vec{u}_{\mathrm{dyn}}$ is the allowed relative overlap. This usually yields time step sizes in the range of $[10^{-6}, 10^{-4}]$s for realistic scenarios. As the step size in implicit schemes is allowed to be several orders of magnitude higher than in explicit schemes, the higher computational effort per step is easily justified. Implicit integration schemes are usually implemented as predictor corrector (PC) schemes, estimating and improving the value at time $t + \Delta t$. Due to the initially unknown acceleration or force value at time $t + \Delta t$, the predictor step is an explicit estimate. With this estimate the right hand side of the equations of motion can be evaluated by neighborhood search and contact evaluation in order to improve the estimate in the corrector. However these right hand side evaluations are especially expensive if several corrector steps are needed, or lower time steps are required due to demanded higher frequency result accuracy. Furthermore, the explicit predictor step potentially calls for more corrector steps, than an implicit predictor would.
Summarizing the state of the art, implicit integrators like the NEWMARK-β scheme [6] are superior to explicit schemes, at the cost of higher computational effort per step. Addressing the shortcomings of state of the implicit integrators this article will present an integration scheme, that approaches the per step performance of an explicit scheme while having the stability conditions and advantages of implicit schemes.

2 INTEGRATION SCHEME

In this section the integration scheme will be derived. Therefore the single steps yielding in an implicit scheme with implicit predictor but without the right hand side evaluations are explained. As a predictor corrector scheme is used to implement the algorithm, x_n denotes the value at iteration step n and index m denotes the converged value.

2.1 General Scheme

As a general basis of the novel integration scheme, the well known NEWMARK-β scheme [6] is enhanced. The NEWMARK scheme is given as follows:

$$\ddot{\vec{x}}(t+\Delta t) = \frac{\vec{F}_\mathrm{c}(t+\Delta t)}{m_\mathrm{p}} \tag{3}$$

$$\dot{\vec{x}}(t+\Delta t) = \dot{\vec{x}}(t) + \Delta t\Big((1-\gamma)\cdot\ddot{\vec{x}}(t) + \gamma\cdot\ddot{\vec{x}}(t+\Delta t)\Big) \tag{4}$$

$$\vec{x}(t+\Delta t) = x(t) + \Delta t\cdot\dot{\vec{x}}(t) + \Delta t^2\Big((\frac{1}{2}-\beta)\cdot\ddot{\vec{x}}(t) + \beta\cdot\ddot{\vec{x}}(t+\Delta t)\Big) \tag{5}$$

with $\vec{F}_\mathrm{c}(t+\Delta t), m_\mathrm{P}$ the contact forces and the particles mass, furthermore β and γ are the parameters of the NEWMARK scheme respectively. For the common choice of $\beta = 0.25$, $\gamma = 0.5$ the scheme is unconditionally stable in case of continuous forces and conditionally stable given Eq. 2 for non-continuous contact forces. This scheme can be implemented using an explicit predictor and thereafter improving the estimates by repeated right hand side evaluations at the estimated positions yielding new position estimates (see [4] for algorithm).

2.2 Predictor

In order to yield an implicit predictor step, the force or acceleration at time $(t+\Delta t)$ is needed. As the scheme especially targets the simulation of dense granular packages, the assumption of constant jolt $\frac{\mathrm{d}^3\vec{x}}{\mathrm{d}t^3}$:

$$\frac{\mathrm{d}^3\vec{x}}{\mathrm{d}t^3}(t) = \left.\frac{\mathrm{d}\ddot{\vec{x}}_m}{\mathrm{d}t}\right|_{(t-\Delta t)}^{t} \tag{6}$$

$$\frac{\mathrm{d}^3\vec{x}}{\mathrm{d}t^3}(t+\Delta t) = \frac{\mathrm{d}^3\vec{x}}{\mathrm{d}t^3}(t) \tag{7}$$

$$\frac{\mathrm{d}^3\vec{x}}{\mathrm{d}t^3}(0) = 0 \tag{8}$$

is made for the acceleration estimate, using the acceleration $\ddot{\vec{x}}_m$ at time t gathered by a single right hand side evaluation. As this estimate is calculated using the current step t and the previous step $t-\Delta t$, it is called left hand estimate and will have the upper index l throughout the paper. Thus the acceleration yields:

$$\ddot{\vec{x}}(t+\Delta t) = \ddot{\vec{x}}(t) + \int_t^{(t+\Delta t)} \left.\frac{\mathrm{d}^3\vec{x}}{\mathrm{d}t^3}\right|_{(t-\Delta t)}^{t} \mathrm{d}t \tag{9}$$

Using Eq. 4 and 9 a left hand velocity $\dot{\vec{x}}_0^l(t+\Delta t)$ estimate is calculated. In order to improve the estimate a right hand approximation is calculated using the assumption of

$$\frac{\mathrm{d}^3\vec{x}}{\mathrm{d}t^3}(t+2\Delta t) = \frac{\mathrm{d}^3\vec{x}}{\mathrm{d}t^3}(t+\Delta t) \tag{10}$$

as well as taking into account a possible change of sign in the velocity during the next step. The coverage of the change of sign is important, as for most force laws in DEM enlarging forces are emerging in approaching particle pairs, but forces are lowering during departure. If the change of sign is not regarded, the force in the consecutive step is overestimated, especially for larger step sizes, leading to non precise results of the corrector. Using $\dot{\vec{x}}_0^l(t+\Delta t)$ and the HADAMARD Product $\circ$ this yields:

$$\ddot{\vec{x}}_0^r(t+\Delta t) = \left(\ddot{\vec{x}}_0^l(t+\Delta t) + \gamma\Delta t \cdot \mathrm{sign}\Big(\dot{\vec{x}}_0^l(t+\Delta t) \circ \dot{\vec{x}}_m(t)\Big) \circ \int_{(t+\Delta t)}^{(t+2\Delta t)} \frac{\mathrm{d}\ddot{\vec{x}}_0}{\mathrm{d}t}\bigg|_t^{(t+\Delta t)} \mathrm{d}t \right) \tag{11}$$

As $\ddot{\vec{x}}_0^r(t+\Delta t)$ is a result of a velocity prediction at $(t+\Delta t)$ and $(t+2\Delta t)$, this yields in γ as a weight factor for the jolt. As the last step in the predictor operation, a centered estimate $\{\vec{x}_0^c(t+\Delta t), \dot{\vec{x}}_0^c(t+\Delta t), \ddot{\vec{x}}_0^c(t+\Delta t)\}$ is calculated:

$$\ddot{\vec{x}}_0^c(t+\Delta t) = (1-\alpha)\cdot\ddot{\vec{x}}_n^l(t+\Delta t) + \alpha\cdot\ddot{\vec{x}}_n^r(t+\Delta t) \tag{12}$$

$$\dot{\vec{x}}_0^c(t+\Delta t) = \dot{\vec{x}}_m(t) + \Delta t\Big((1-\gamma)\cdot\ddot{\vec{x}}_m(t) + \gamma\cdot\ddot{\vec{x}}_0^c(t+\Delta t)\Big) \tag{13}$$

$$\vec{x}_0^c(t+\Delta t) = \vec{x}_m(t) + \Delta t\cdot\dot{\vec{x}}_m(t) + \Delta t^2\left(\left(\frac{1}{2}-\beta\right)\cdot\ddot{\vec{x}}_m(t) + \beta\cdot\ddot{\vec{x}}_0^c(t+\Delta t)\right) \tag{14}$$

Thereby α is introduced in addition to the NEWMARK coefficients β and γ to allow for weighting towards left or right handed estimate. However the default recommendation of $\alpha = 0.5$ yields in the exactly centered acceleration. For the full PC-scheme, the choice of $\beta = 0.25$ and $\gamma = 0.5$ follows NEWMARK's suggestion. Yet, if the predictor is used without the corrector in order to save computational effort, the choice of $\gamma \approx 0.7$ is advised in order to introduce stability by moderate numerical damping. This use is only advisable if the force law itself cannot be covered by the corrector. Accordingly, if speed-up is crucial, it is better to use the left hand estimate predictor only, knowingly sacrificing the knowledge about possible change of sign in the velocity during the next step.

2.3 Force-law based Corrector

As the corrector is utilized to improve the estimates in the predictor to a valid forecast of the values at time $(t+\Delta t)$ it is iterated either till convergence or a maximum number of iterations m is reached. Thereby the acceleration estimate is improved using an assessment

of the force law used. In general this yields:

$$\ddot{\vec{x}}_n^c(t+\Delta t) = \ddot{\vec{x}}_m(t) + \int_t^{(t+\Delta t)} \left.\frac{\mathrm{d}^3\vec{x}}{\mathrm{d}t^3}\right|_t^{(t+\Delta t)} \mathrm{d}t \tag{15}$$

The future value of $\left.\frac{\mathrm{d}^3\vec{x}}{\mathrm{d}t^3}\right|_t^{(t+\Delta t)}$ is not assessable without rerunning neighborhood search and contact force evaluation. Thus it has to be calculated based on the previous iterations of the prediction, as well as the knowledge about the force law. In order to include the commonly used elastic normal forces in DEM an equivalent stiffness $\overline{c}(t)$ to estimate the next force can be defined as:

$$\overline{c}(t) = \nabla \circ \ddot{\vec{x}}\Big|_{\vec{x}_m(t-\Delta t)}^{\vec{x}_m(t)} \tag{16}$$

Evaluating $\ddot{\vec{x}}_n^c(t+\Delta t)$ using the elastic law and $\overline{c}(t)$ then yields:

$$\ddot{\vec{x}}_n^c(t+\Delta t) = \ddot{\vec{x}}_m(t) + \xi \int_{\vec{x}_m(t)}^{\vec{x}_{n-1}(t+\Delta t)} \left(\nabla \circ \ddot{\vec{x}}\Big|_{\vec{x}_m(t-\Delta t)}^{\vec{x}_m(t)}\right) \mathrm{d}\vec{x} \tag{17}$$

with $\xi \in [0,1]$ being a weighting factor dependent on the force law used, but usually chosen to be one. This forecast of acceleration is valid for both linear and non-linear force laws, including friction. As the contact itself needs to be covered by a sufficient number of time steps, changes in equivalent stiffness are sufficiently low even for non-linear force laws. After assessing the acceleration, the velocity and position are updated accordingly:

$$\dot{\vec{x}}_n(t+\Delta t) = \dot{\vec{x}}_m(t) + \Delta t\Big((1-\gamma)\cdot\ddot{\vec{x}}_m(t) + \gamma\cdot\ddot{\vec{x}}_n^c(t+\Delta t)\Big) \tag{18}$$

$$\vec{x}_n(t+\Delta t) = x_m(t) + \Delta t\cdot\dot{\vec{x}}_m(t) + \Delta t^2\left(\left(\frac{1}{2}-\beta\right)\cdot\ddot{\vec{x}}_m(t) + \beta\cdot\ddot{\vec{x}}_n^c(t+\Delta t)\right) \tag{19}$$

As the algorithm tends to converge within a few steps, using $m \in [2,5]$ is a good choice for fixed iterations without the need to control convergence saving computational effort.

Integration of the Rotations

Integration of the rotations of the six DOF particles is carried out analogous to the translation. The only difference is due to the use of quaternions at rotation-level.

2.4 Automatic Step Size Control

In order to allow the integrator to adapt its step size as well as number of iteration to the current behaviour of the solution, a time step size control is implemented.

Convergence of Corrector Loop

In order to allow the number of iteration to be controlled by convergence of the corrector, the maximum relative error of the acceleration $\varepsilon_{\mathrm{it}}(t+\Delta t, n)$ between two iterations is used. If $\varepsilon_{\mathrm{it}}(t+\Delta t, n) < \eta_{\mathrm{rel}}$ is true, the corrector iteration cycle is converged. $\varepsilon_{\mathrm{it}}(t+\Delta t, n)$ derives to:

$$\varepsilon_{\mathrm{it}}(t+\Delta t, n) = \sum_{i=1}^{k} \left(k\Delta t^2 \cdot \frac{\max\left(\left| {}^{i}\ddot{\vec{x}}_n^c(t+\Delta t) - {}^{i}\ddot{\vec{x}}_{n-1}^c(t+\Delta t) \right| \right)}{2 \cdot \left(\sum_{i=1}^{k} \left| {}^{i}\ddot{\vec{x}}_n^c(t+\Delta t) - {}^{i}\ddot{\vec{x}}_{n-1}^c(t+\Delta t) \right| + \eta_{\mathrm{abs}} \right)} \right) \tag{20}$$

with k the number of particles and η_{abs} an absolute tolerance value. This tolerance especially accounts for zero error in free falling particles.

Control of Time Step Size

The time step size is either controlled by the actual error $\varepsilon_r(t)$ of the acceleration estimation during the current step or by lowering the step if the corrector loop did not converge. The error is therefore derived to:

$$\varepsilon_r(t) = \sum_{i=1}^{k} \left(k\Delta t^2 \cdot \frac{\max\left(\left| {}^{i}\ddot{\vec{x}}_m^c(t) - {}^{i}\ddot{\vec{x}}^{\mathrm{cd}}(t) \right| \right)}{2 \cdot \left(\sum_{i=1}^{k} \left| {}^{i}\ddot{\vec{x}}_m^c(t) - {}^{i}\ddot{\vec{x}}^{\mathrm{cd}}(t) \right| + \eta_{\mathrm{abs}} \right)} \right) \tag{21}$$

with ${}^{i}\ddot{\vec{x}}_m^c(t)$ being the predicted acceleration of every particle i and ${}^{i}\ddot{\vec{x}}^{\mathrm{cd}}(t)$ the actual acceleration derived at the beginning of the next step using neighborhood search and contact force evaluation. $\varepsilon_r(t)$ itself actually describes the effect of the acceleration error on the accuracy of the calculated position at the end of the time step. The quotient $\text{ϑ}(t)$ of the relative tolerance η_{rel} and $\varepsilon_r(t)$:

$$\text{ϑ}(t) = \frac{\eta_{\mathrm{rel}}}{\varepsilon_r(t)} \tag{22}$$

is then used as input for the step size control law. This yields in adequate increase in time step in case of lower errors, i.e. lower number of changes in the contact neighbourhood.

3 APPLICATION & RESULTS

In order to verify the applicability of the integration scheme in DEM and contact dynamics, two example applications are evaluated in this section - a simple bouncing sphere and a piling experiment. Thereby the simple example will also be used in order to analyze energy conservation of the scheme. Prior to those applications the used force law is introduced. The integration scheme was also initially verified using the harmonic oscillator, which will not be shown in this paper, as the focus is on worst-case examples.

3.1 Contact Model

In order to show that the integrator does not only work for linear contact forces, but also non-linear laws including damping, the widely used HERTZian contact law is utilized instead of a linear law. Using the adaption for DEM shown in [5] the resultant force in case of overlap evaluates to

$$\vec{F}_{\mathrm{N}}^{nm} = \left(\frac{2E}{3(1-\nu^2)} \sqrt{r_{\mathrm{C}}^{nm} |\vec{\delta}^{nm}|^3} \right) \vec{n}_c^{\,n} + k_{\mathrm{Nmin}}^{nm} \dot{\vec{\delta}}^{nm} \tag{23}$$

with YOUNG's Modulus E, POISSON's Ratio ν, r_{C}^{nm} the mean particle radius of particles m and n and $\vec{\delta}^{nm}$ the overlap. $\vec{n}_c^{\,n}$ and $k_{\mathrm{Nmin}}^{nm} \leq 0$ are the contact normal for each particle and the damping coefficient respectively. In the first tests, only the normal force will be used. In the piling experiments shown later in the paper, frictional forces and rotational DOFs are added in order to check the applicability of the proposed integrator for general DEM problems. In order to model friction, the approach shown by LICHTENHELDT [1] is used:

$$\vec{F}_{c\mathrm{T}}^{nm} = c_{\mathrm{T}}^{nm} \cdot \vec{\delta}_{\mathrm{T}}^{nm} \cdot \mathrm{sign}\left(\vec{\delta}_{\mathrm{T}}^{nm} \cdot \dot{\vec{\delta}}_{\mathrm{T}}^{nm} \right) + k_{\mathrm{T}}^{nm} \cdot \dot{\vec{\delta}}_{\mathrm{T}}^{nm} \tag{24}$$

$$\vec{F}_{\mathrm{T}}^{nm} = \begin{cases} \vec{F}_{c\mathrm{T}}^{nm} & \forall\ |\vec{F}_{c\mathrm{T}}^{nm}| \leq |\vec{F}_{\mathrm{N}}^{nm}| \cdot \tan(\phi_{\mathrm{h}}) \ \wedge\ |\dot{\vec{\delta}}_{\mathrm{T}}^{nm}| \leq v_{\mathrm{Tmin}}^{nm} \\ \vec{F}_{\mathrm{N}}^{nm} \cdot \tan(\phi_{\mathrm{g}}) \cdot (\dot{\vec{\delta}}_{\mathrm{T}}^{nm})_0 & \forall\ |\vec{F}_{c\mathrm{T}}^{nm}| > |\vec{F}_{\mathrm{N}}^{nm}| \cdot \tan(\phi_{\mathrm{h}}) \ \vee\ |\dot{\vec{\delta}}_{\mathrm{T}}^{nm}| > v_{\mathrm{Tmin}}^{nm} \end{cases} \tag{25}$$

whereas $\phi_{\mathrm{g,h}}$ are the friction coefficients for sliding and sticking and c_{T}^{nm}, k_{T}^{nm} are the regularization stiffness and damping respectively. For rotations a commonly used rolling friction is added in order to provide proper rolling behaviour.

3.2 Bouncing Spheres

The first example models two spheres bouncing on each other perfectly centered. Therefore the lower sphere is fixed, while the upper sphere is free to fall until it contacts the second one. This example serves as benchmark in terms of energy conservation in cases with opening and closing contacts. These situations are worst-case for the scheme, as the impact and thus the sudden change in acceleration is not predicted beforehand, but only the step after the impact occurred. This makes this simple example more delicate in terms of verification compared to the harmonic oscillator. The example is fully conservative, thus no damping or friction is present.
The integration scheme has been tested for different time step sizes and automatic time stepping as shown in Fig. 1 (left). It can be seen, that even for large time steps in the sense of contact mechanics, stable solutions are found, i.e. no energy is generated. Only for a step size of $\Delta t = 10^{-3}$s there is a decrease in potential energy, as the integrator tends to damp the system numerically for arbitrarily high step sizes.

Furthermore it is worth mentioning, that the NEWMARK reference scheme showed an increase in energy for $\Delta t = 10^{-3}$s already.

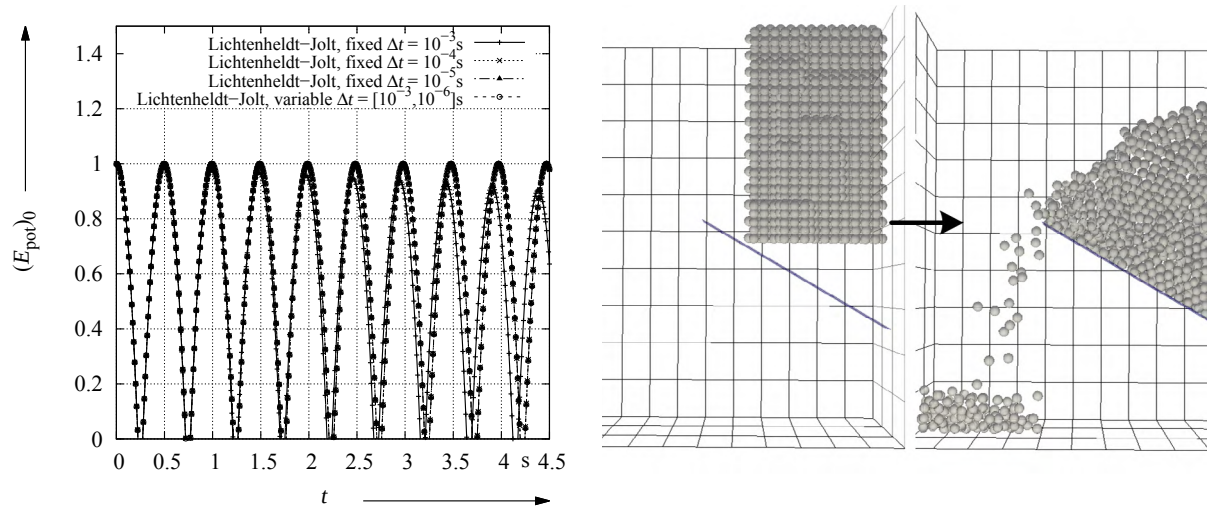

Figure 1: Normalized potential energy for the upper bouncing sphere for different time step sizes (left), Piling scenario with box and tilted plane visualized (right)

3.3 Piling Experiment

The piling scenario has been chosen as it features both, dense and flow states of granular matter making it an ideal test case for the proposed scheme. As shown in Fig. 1 (right), the scenario consists of a particle package dropping on an inclined plane creating a particle flow in the surrounding box until the pile is settled at the angle of repose. In the first test only normal forces are applied and the damping is set to 20% of critical damping. The same scenario is executed with the jolt-based and the reference integrator, whereas the NEWMARK scheme runs with $\Delta t = 10^{-5}$s and three iterations. For the jolt-based scheme both fixed step (three iterations) and variable step simulations are carried out dependent on the scenario. In the second test case frictional forces and rotational DOFs are added.

Accuracy

In Fig. 2 the jolt-based integrator is represented by gray particles, the NEWMARK integrator by green particles (note that the particles are scaled down for visibility) meshed via delaunay triangularization. Both results have been superimposed in Fig. 2 in order to allow for proper comparison. As it can be seen in the pictures, most of the gray particles are contained by the mesh, especially for the dense parts of the flow. Especially for the upper portion of particles situated in the pile there is almost no visible deviation. These qualitative findings are supported by the plotted total energy in Fig. 4 on the left. The jolt-based integrator shows slightly higher dissipation compared to the NEWMARK reference, but shows 2.11% of energy error, while increasing simulation speed.
In order to proof the applicability of the introduced scheme, it is tested with frictional contacts. Contact coefficients are chosen correspondent to [1]. Figure 3 shows the animated comparison as for the non-frictional case for fixed step simulations using $\Delta t = 10^{-5}$s. It

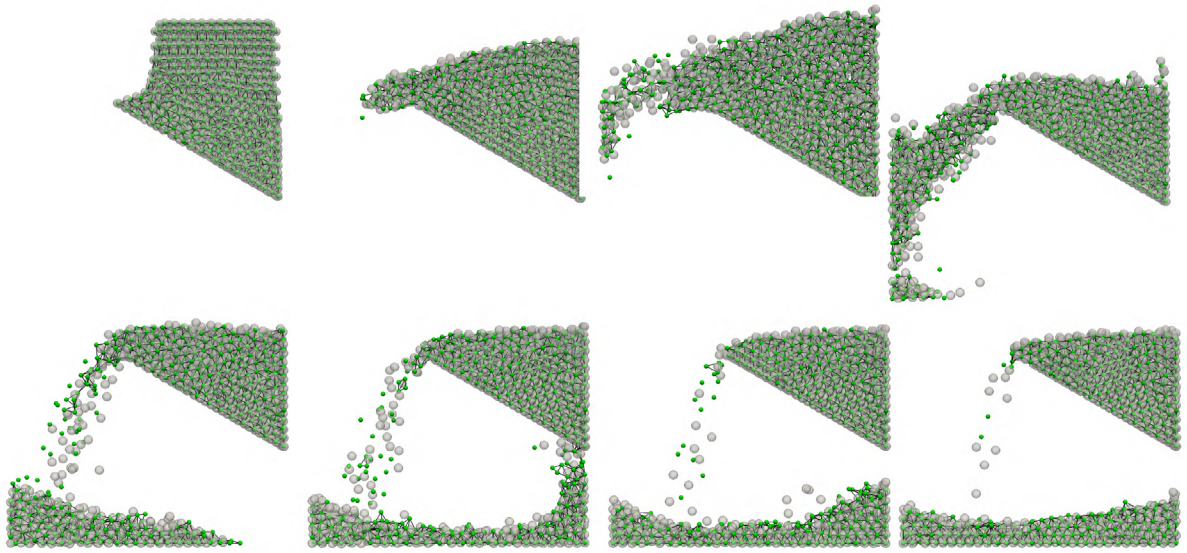

Figure 2: Piling for jolt-based (gray particles) and reference NEWMARK integrator (green meshed particles) for non-frictional contact

can be seen that the gray particles are again well contained in the mesh, however in the beginning the jolt-based integrator slightly lower volume in the upper pile and thus higher volume flow to the surrounding box. Given these slight variations it is still possible to capture the correct angle of the pile in every frame. The later frames with less particle movement are in even better agreement regarding the pile and the dense areas. Especially in the end of the simulation the same angle of repose is reached, i.e. the shear strength is covered correctly. Similar to the non-frictional piling, the frictional scenario also shows good agreement of the total energy compared to the reference integrator. Figure 4 shows the fixed step, as well as the variable step case. It can be seen, that the fixed step version is more precise, as the automatic time stepping tends to chose as high step sizes as possible in order to improve computational efficiency (see Figure 5 left). Regarding the relative error with respect to the reference scheme, both are well below 5% of error, whereas the fixed version is even below 2.2%. This result has been a surprise, as the corrector part of the scheme does not cover any kind of frictional or dissipative force but assumes a stiffness only. The fact that the forces are accurately assumed can also be seen in Fig. 5 right. The graph shows the maximum relative error between the converged prediction value $\ddot{\vec{x}}_m(t + \Delta t)$ of the last time step and the actual acceleration determined by contact detection in the current step. Most of the values are in the range of the desired value of 10^{-8}. All the values above have only minor influence on the results as they are in the same order of magnitude as the desired value and correspond to single particles changing their contact state. By activating back-stepping in the algorithm, these overshoots can be omitted while sacrificing some of the performance gain.

Performance

As in the previous section the new scheme showed sufficient accuracy, performance is compared to the reference solver accordingly. Therefore the same set of simulations as for the frictional piling case is used. Table 1 shows the results of the comparison. The

Table 1: Performance comparison of the integrators

Integrator	step size [s]	num. iterations	normalized time used []
NEWMARK	10^-5	3	1
LICHTENHELDT-Jolt	10^-5	3	0.5
LICHTENHELDT-Jolt	$[10^-6, 10^-2]$	$[1, 10]$	0.481
LICHTENHELDT-Jolt	$[10^-6, 10^-2]$	3	0.254

simulation time has been normalized to the NEWMARK result to allow easier comparison. The fixed step, fixed iteration jolt integrator is already two times faster than the reference. Sacrificing single percents of accuracy performance can be increased up to four times the speed of the reference integrator, by running step size controlled with fixed number

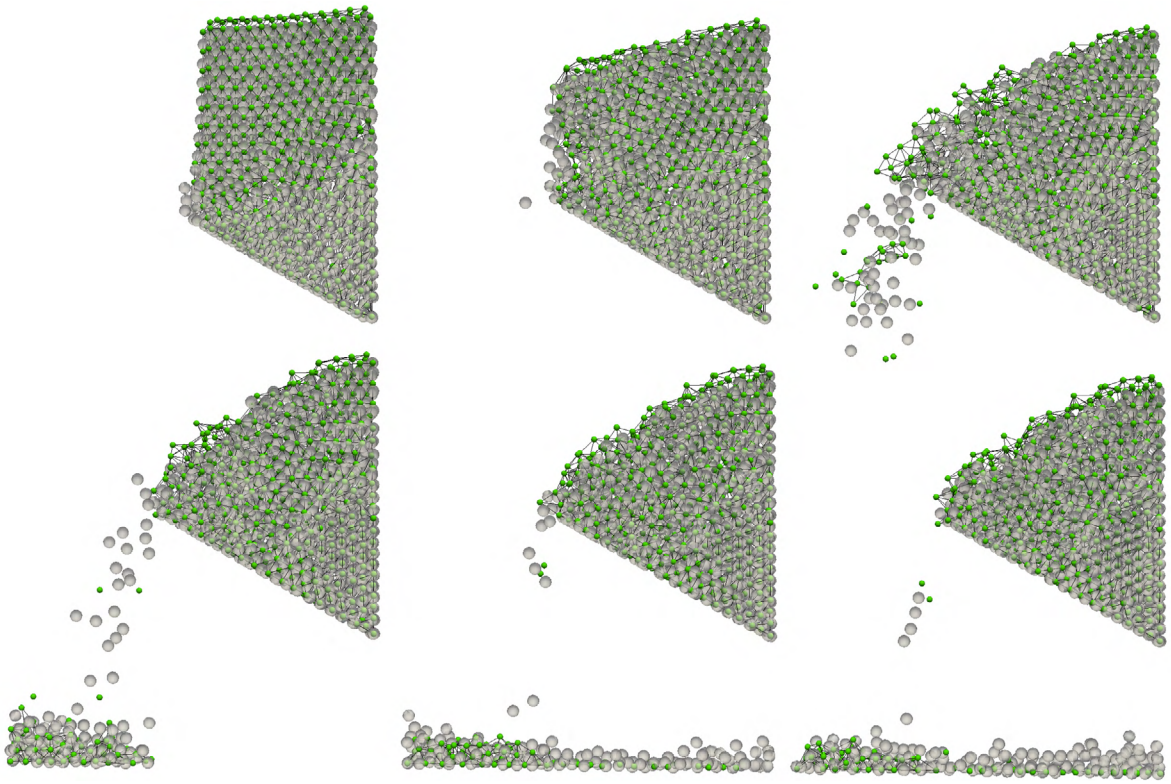

Figure 3: Piling for jolt-based (gray particles) and reference NEWMARK integrator (green meshed particles) for frictional contact

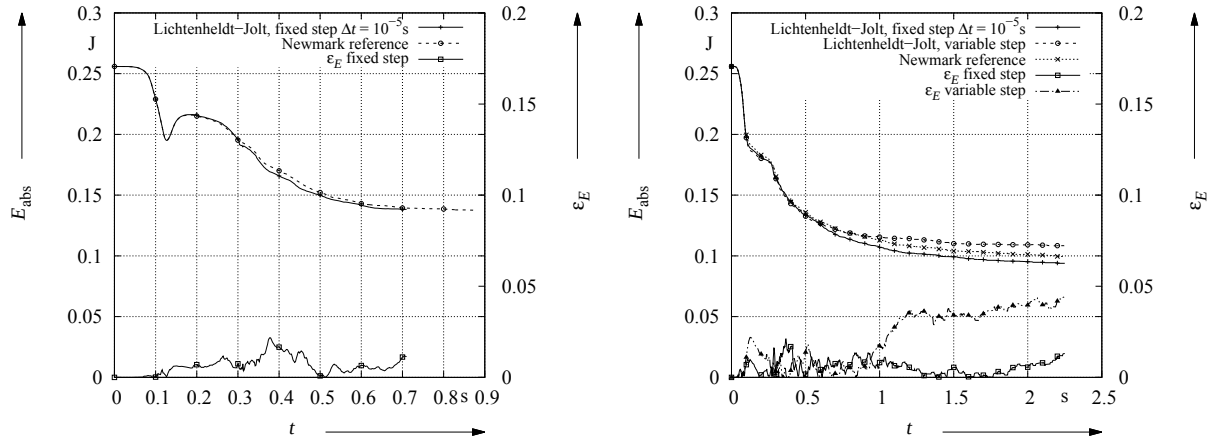

Figure 4: Total energy and relative energy error for the proposed and reference integrator for non frictional piling (left) and piling featuring friction (right)

of corrector iterations. Given the negligible loss in accuracy and the correctly covered shear strength of the material the integrator is a good alternative to the NEWMARK scheme whenever it comes to performance or software architecture. Compared to explicit integrators, both schemes showed great advantages as the time step could be chosen several orders of magnitudes higher.

4 CONCLUSION

In this article a novel implicit integration scheme has been proposed. On the basis of the NEWMARK integration scheme it uses a jolt-based approximation for the accelerations at the next time step. It specially targets particle simulations, as renewed contact detection and force evaluation at every corrector iteration are costly. Discarding these by using the

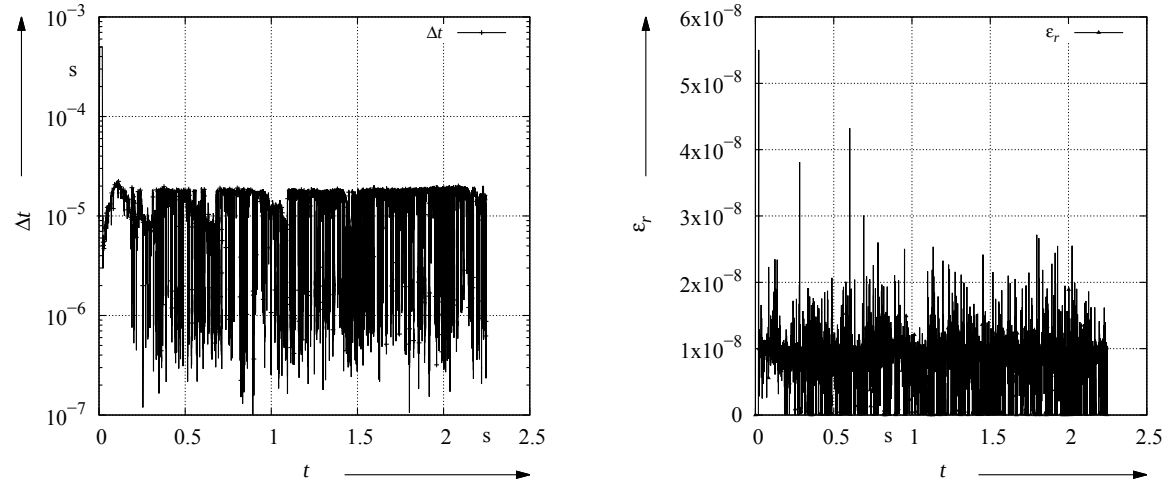

Figure 5: Time step size as chosen by the controller (left) and relative force error of the jolt-based prediction compared to the evaluated force (right)

approximation, the scheme also simplifies the architectural aspects of the code, making it easy to implement in any software featuring explicit integrators, which would not allow for renewed force calculation otherwise. Hence the scheme will also be used in DLR's GPU based simulation framework [7].
In the first sample applications it was shown, that the scheme is numerically stable for contact problems even up to arbitrarily high time steps and even for too large step sizes the integrator shows numerical damping instead of instability, making it most suitable for particle simulations. The scheme's accuracy has been verified using piling simulations and showed that for two times faster computation only 2.1% of error are arising. Tolerating negligibly low 4.4% of error results in an even higher speed up of a factor of four.
Given the advantages in performance, stability, implementation, architectural aspects and its direct applicability to GPU-computing paradigms, the LICHTENHELDT-Jolt integration scheme poses an interesting alternativ to both, common implicit and especially explicit schemes in Discrete Element Method.

ACKNOWLEDGEMENTS

Special thanks go to Simon Kerler, who's work required a simple efficient and implicit integration scheme and thus inspired this work.

REFERENCES

[1] R. Lichtenheldt. A novel systematic method to estimate the contact parameters of particles in discrete element simulations of soil. In *4th International Conference on Particle-based Methods - Particles 2015, pp 430-441, ISBN:978-84-944244-7-2, Barcelona*, 2015.

[2] V. Smilauer and B. Chareyre. Yade dem formulation. Technical report, Yade Documentation, The Yade Project, 1st ed., 2010. http://yade-dem.org/doc/formulation.html.

[3] F. Fleissner. Dokumentation, template-files und beispiele zum programmpaket "pasimodo". Template files, Inpartik & Universität Stuttgart, 2012.

[4] F. Fleissner. *Parallel Object Oriented Simulation with Lagrangian Particle Methods*. PhD thesis, Universität Stuttgart, 2010.

[5] R. Lichtenheldt. *Lokomotorische Interaktion Planetarer Explorationssysteme mit weichen Sandböden - Modellbildung und Simulation*. PhD thesis, Ilmenau University of Technology, ISBN 978-3-8439-2704-8, 2016.

[6] N.M. Newmark. A method of computation for structural dynamics. *Journal of the Engineering Mechanics Division*, pages 67–94, 1959.

[7] S. Kerler. Collision-based Particle Simulations on GPUs for Planetary Exploration Systems. Master's thesis, Augsburg University, 2017.